Reaction Chemistry & Engineering

Linking fundamental chemistry and engineering to create scalable, efficient processes

Accepted Manuscript

This article can be cited before page numbers have been issued, to do this please use: M. Blair, M. Molaei Chalchooghi, R. Cox and D. I. Gerogiorgis, *React. Chem. Eng.*, 2025, DOI: 10.1039/D5RE00082C.

ROYAL SOCIETY OF CHEMISTRY

rsc.li/reaction-engineering

View Article Online
DOI: 10.1039/D5RE00082C

Reaction Kinetics for the Synthesis of an Anti-cancer Drug (Adavosertib) Precursor

Matthew Blair[a], Mazaher M. Chalchooghi[b], Robert J. Cox[b], Dimitrios I. Gerogiorgis[a,*]

[a]Institute for Materials and Processes (IMP), School of Engineering, University of Edinburgh, The King's Buildings, Edinburgh, EH9 3FB, United Kingdom

[b]Chemical Development, Pharmaceutical Technology and Development, Operations, AstraZeneca, Macclesfield, SK10 2NA, United Kingdom

ABSTRACT

The development of kinetic models which can accurately describe drug synthesis reactions is an important part of process design in the pharmaceutical industry. Correctly identifying these models can be difficult, however, since the reaction pathways used to manufacture new pharmaceutical compounds are often extremely complex. Consequently, many kinetic modelling and parameter estimation tools have been developed in recent years to allow drug manufacturers to test and compare a variety of reaction models before selecting the one which provides the best predictions. In light of this, in the present paper, we have used a multistart parameter estimation code (written in MATLAB®) to parameterise a range of kinetic models developed to describe the synthesis of an important intermediate required for the production of a new anti-cancer drug, Adavosertib (AZD1775). Further to this, we have used Akaike and Bayesian Information Criteria to rank these models based upon their complexity and ability to reflect real-world observations.

1. INTRODUCTION

Since 2005, public spending on anti-cancer drugs has steadily increased across Europe (Figure 1a) and the United States; leading to a total global spending of 150 billion USD in 2020 [1, 2]. Whilst some of this spending can be attributed to rising incidence rates of various cancer around the world [2-6] (with 18.1 million new cases and 10 million deaths reported in 2020 alone [7]), it is clear that rising drug prices have helped to shape this landscape (Figure 1b). Consequently, pharmaceutical companies must find a way to reduce the price of their medications if they hope to prevent treatments from becoming unaffordable in the future [1, 2].

In order to accomplish this, however, drug manufacturers must first find a way to intensify their manufacturing processes. Moreover, they must do so whilst minimising experimentation so as to not simply inflate costs elsewhere in their pipeline. It has, therefore, been suggested by many authors [8-16] that fit-for-purpose process models should be developed which can be used to describe the different unit different operations involved in pharmaceutical processes. The reason being that, once these models are correctly parameterised, they can provide an efficient way to visualise and optimise processes. This has already been demonstrated by Jolliffe et al. [15], Diab et al. [8], and Cuthbertson et al. [17] for ibuprofen, diphenhydramine and amoxicillin, respectively.

In response to this, numerous studies have been published in recent years covering the importance of developing and parameterising kinetic models for chemical synthesis [11, 18-36] and crystallisation processes [37, 38]; with the former receiving particular attention (Table 1). For example, in 2021, Schenk et al. [39] demonstrated how parameter estimation tools can be used to compare different kinetic models

View Article Online
DOI: 10.1039/D5RE00082C

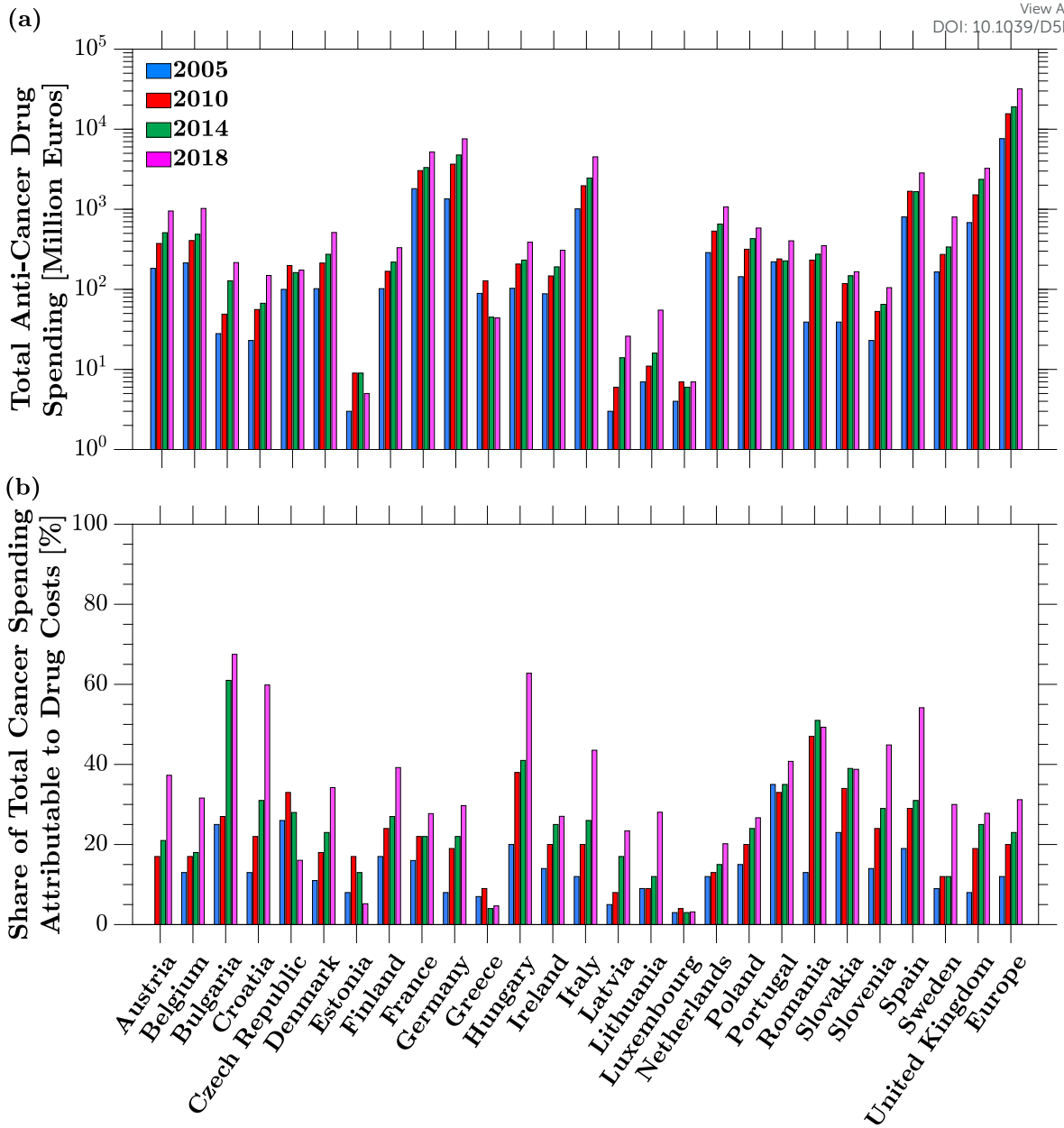

Figure 1. Anti-cancer spending in Europe 2005-2018 (data from [2, 3]). (a) Spending on anti-cancer drugs; (b) contribution of drug costs towards total spending.

available to describe drug synthesis processes; using the production of an asymmetrical urea compound required to manufacture various active pharmaceutical ingredients (APIs) as a case study. Meanwhile, in 2016, Grom et al. [22] showed that computational modelling techniques could be used to study the reaction mechanisms underpinning Lorcaserin synthesis (a complicated reaction network, consisting of 27 reaction steps and 15 chemical species); ultimately, leading to the robust development of a temperature-dependent kinetic model containing 29 parameters. Likewise, various studies have been conducted to show how kinetic modelling can be used to assess the benefits of different manufacturing techniques such as batch and continuous processing [12, 40]. Including the work of Kraus et al. [41], which considered the eco-friendly of carbamazepine from urea and iminostilbene. As a result of these efforts, various software packages now exist which can be used to conduct this type of work; notable instances of which are summarised in Table 2.

View Article Online
DOI: 10.1039/D5RE00082C

Table 1. Summary of various reaction modelling and kinetic parameter estimation studies conducted for different APIs and drug precursors in the literature.

API/Precursor	Condition Treated	Study Outcomes	Software	Ref.
Carbamazepine	Epilepsy	Kinetic model & Arrhenius rate law	MATLAB	[41]
Unspecified	Unspecified	Kinetic model & isothermal rate constants	KIPET	[39]
Lorcaserin	Obesity	Kinetic model & Arrhenius rate law	–	[22]
Lomustine	Brain tumours, Hodgkin's lymphoma	Kinetic models, isothermal rate constants	MATLAB	[18]
Osimertinib Intermediate	Non-small cell lung cancer	Kinetic model & Arrhenius rate law	Dynochem	[19]
Carfilozomib Intermediate	Myeloma	Kinetic model & Arrhenius rate law	Dynochem	[20]
Merestinib Intermediate	Biliary tract & non-small cell lung cancer	Kinetic model & isothermal rate constants	–	[21]
Paracetamol	Moderate pain, fevers	Kinetic model & isothermal rate constants	MATLAB	[23]
Metoprolol	High blood pressure	Kinetic model & isothermal rate constants	MATLAB	[23]
Unspecified	Unspecified	Kinetic model & isothermal rate constants	KIPET	[24]
Ibuprofen	Moderate pain, fevers, inflammation	Kinetic model & isothermal rate constants	MATLAB	[25]
Diphenhydramine	Hay fever, common cold, short-term insomnia	Kinetic model & isothermal rate constants	MATLAB	[8]
Nevirapine	HIV	Arrhenius rate law	MATLAB	[11]
Aziridines (building block)	Cancer therapies (Mitomycin, Azinomycin)	Arrhenius rate law	gPROMS	[26]
Pyrroles (building block)	Cancer therapies (Sunitinib), pain relief (Ketorolac), heart disease (Atorvastatin)	Kinetic models & Arrhenius rate law	COMSOL Multiphysics	[27]
Abemaciclib	Advanced/metastatic breast cancers	Arrhenius rate law	Dynochem	[28]
Thiazolidine Intermediate	Diabetes	Kinetic model & Arrhenius rate law	–	[29]
Glitazone Intermediate	Diabetes	Kinetic model & Arrhenius rate law	–	[30]
Tryptophol	Insomnia	Kinetic model & Arrhenius rate law	COMSOL	[31]
Dolutegravir Intermediate	HIV	Kinetic model & Arrhenius rate law	COMSOL	[32]

View Article Online
DOI: 10.1039/D5RE00082C

Table 2. Overview of software packages available for kinetic parameter estimation. CT = concentration-time data; AT = absorbance-time data; V = various data forms.

	Software Elements	Required Packages	Input Data	Open Source
Dynochem [42]	• ODE solvers (e.g., Rosenbrock) • Local-optimisation algorithms (e.g., Levenberg-Marquardt) and search tools (e.g., multiple start-point)	• Dynochem	V	✗
MATLAB [43]	• ODE solvers (e.g., Rosenbrock, Runge-Kutta, Variable Step Variable Order solvers) • Various optimisation algorithms (e.g., Levenberg-Marquardt, trust-region-reflective, simulated annealing, Nelder-Mead, genetic algorithm, particle swarm, surrogate polynomial optimisation, pattern search) and search tools (e.g., multiple start-point)	• MATLAB • Global optimisation toolbox	V	✗
gPROMS [44, 45]	• ODE solvers (e.g., DAEBDF, or DASOLV variable step variable order backward differentiation formulae, SRADAU Variable Step Runge-Kutta) • Local-optimisation algorithms (e.g., maximum likelihood) and search tools (e.g., multiple start-point)	• gPROMS Process or Formulated Products	V	✗
SciPy [46]	• ODE solvers (e.g., Runge-Kutta, variable step variable order solvers) • Local-optimisation algorithms (e.g., Nelder-Mead, trust region reflective, Newton-CG, sequential least squares programming)	• Python • SciPy • NumPy	V	✓
KIPET [24, 47, 48]	• ODE solvers (e.g., orthogonal collocation on finite elements) • Local-optimisation algorithms (e.g., maximum likelihood) and search tools (e.g., multiple start-point)	• Python • Pyomo • SciPy • NumPy • KIPET	CT AT	✓
GEKKO [49]	• ODE solvers (e.g., orthogonal collocation on finite elements) • Local optimisation algorithms and Hyperopt search tools (e.g., grid search, random search, tree-structured parzen estimator, adaptive tree-structured parzen estimator)	• Python • GEKKO • NumPy	V	✓
GDOC [33, 35, 36, 50]	• ODE solvers (e.g., CVODES) • Local-optimisation algorithms (e.g., sequential quadratic programming via NPSOL, etc.) and search tools (e.g., branch and bound algorithm coupled with convex relaxation considerations)	• Fortran, C, or C++ • NPSOL • Any ANSI compliant Fortran, C, or C++ compiler	CT	✗
COMSOL [51, 52]	• ODE solvers and optimisation modules (e.g., Optimisation Module, LiveLink™ for MATLAB) • Local-optimisation algorithms (e.g., Levenberg-Marquardt, Bound Optimisation BY Quadratic Approximation)	• COMSOL Multiphysics	V	✗

View Article Online
DOI: 10.1039/D5RE00082C

Alongside this, however, several studies have also been conducted to show how computational modelling can be used to simplify the task of conceptualising and ranking the kinetic models developed for these reactions in the first place [53]. For instance, Tsu et al. [54] recently used Integer Linear Programming (ILP) to identify stoichiometric coefficients for synthetic chemical reactions, whilst August et al. [55] used it to identify promising chemical reaction networks for biological systems. Meanwhile, Taylor et al. [23, 56] and Willis et al. [57] have shown that Mixed Integer Linear Programming (MINLP) can be used to automatically generate and test different rate laws and reaction networks for systems where the reactants, products and intermediates are already known. Ultimately, allowing all feasible unimolecular and bimolecular reactions between different chemical species to be determined autonomously [53, 54, 57]; before leveraging metrics such as the Akaike [23, 56, 58] and Bayesian Information Criterions [59] to identify models which have the simplest structure, yet can accurately predict experimental observations [23, 60].

In light of these efforts, one cancer therapy which would particularly benefit from this type of work is Adavosertib (AZD1775) – an experimental oral medication thought to inhibit tyrosine kinase WEE1 activity during cell signalling, growth and division [61] – since it has shown clinical efficacy as a monotherapy against a range of cancers. Most notably, against non-small cell lung cancer (NSCLC) and pancreatic cancers [62], which together account for over half of all cancer related deaths in Europe today [4]. Though, it has also shown promise as a combinatorial therapy when treating NSCLC, ovarian cancer and leukemia using Sotorasib [63], chemotherapy [62] and Cytarabine [64] as partner therapies.

Considering this, in the present paper we propose a range of kinetic models which can be used to describe the synthesis of an important precursor required for Adavosertib production: AZD1775 Hydroxymethylsulfanyl. No reaction mechanism, nor kinetic model, has been previously proposed for the synthesis of this compound; yet, understanding its production is essential for the cost-effective manufacture of Adavosertib. To complete this work, we have used a simple parameter estimation code written in MATLAB® to parameterise 64 candidate kinetic models; before ranking them based on their complexity and ability to reflect experimental observations. Importantly, each of the models considered have been developed using knowledge of similar reactions.

2. EXPERIMENTAL

To obtain the experimental data required for kinetic modelling, AZD1775 HMS was synthesised from a feedstock of pyrimidine (Pyr) and bromopyridine (PyBr) in the presence of potassium acetate (KOAc); using copper (I) iodide (Cu(I)I) and racemic +/- trans-N,N'-dimethylcyclohexane-1,2-diamine (CyDMEDA) acting as a catalyst and ligand, respectively (Figure 2).

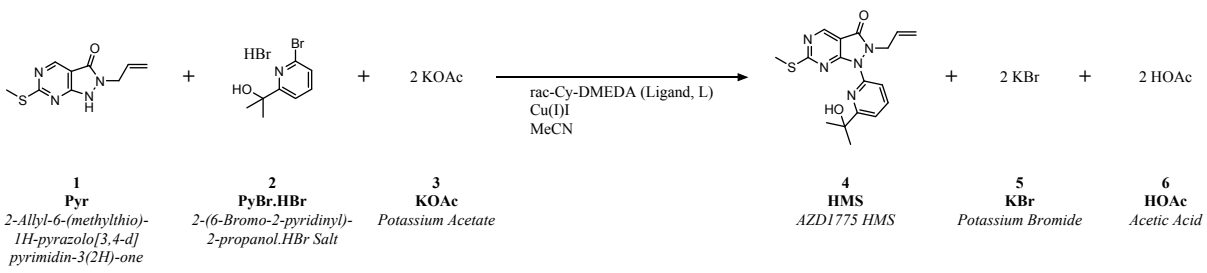

Figure 2. Overall reaction scheme for batch synthesis of AZD1775 HMS.

View Article Online
DOI: 10.1039/D5RE00082C

In order to achieve this, however, it was necessary to first weigh out appropriate amounts of each solid reagent (i.e., Pyr, PyBr, KOAc, Cu(I)I and CyDMEDA) into vials, before purging them with nitrogen. Likewise, it was important to add the reaction solvent (degassed MeCN) to these reagents under inert conditions only. Consequently, an Amigo Chem® workstation (Figure 3) has been used to carry out the synthesis reaction in question; considering a range of reaction temperatures (338.15, 348.15, and 355.15 K) and initial reagent concentrations (c.f. Supplementary Information, Table S1). Alongside this, however, High Performance Liquid Chromatography (HPLC) has been used to determine the concentration-time profile of each reagent during these reactions (hereafter, referred to as experiments a-n); measuring the concentration of species Pyr, PyBr, PyI and HMS over the course of the reaction. Though it is important to note that, in the final experimental run (i.e., experiment 'n'), Pyr concentration was not recorded.

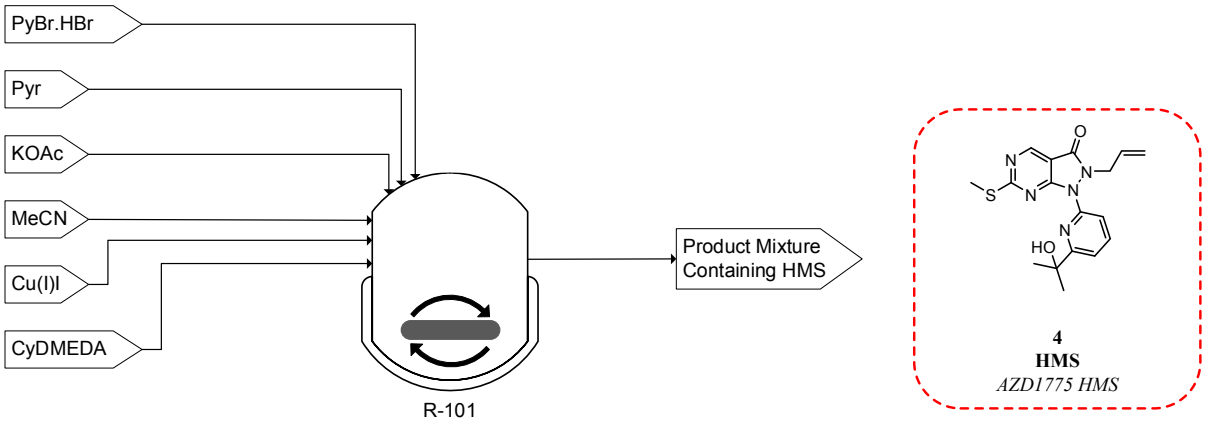

Figure 3. Schematic representation of magnetically stirred Amigo Chem® batch reactor used for AZD1775 HMS synthesis.

Properties of key chemicals used to complete this work are provided in Table 3.

Table 3. Properties of compounds used in AZD1775 HMS synthesis ([a] = [65]; [b] = [66]).

Species	Role	#CAS	Chemical Formula	M [g mol^{-1}]	T_{bp} [K]	T_{mp} [K]
Pyr	Reagent	955368-90-8	$C_9H_{10}N_4OS$	222.27	671.05[a]	–
PyBr · HBr	Reagent	–	$C_8H_{11}Br_2NO$	296.99	–	–
PyBr	Reagent	638218-78-7	$C_8H_{10}BrNO$	216.08	546.35[a]	339.36[a]
HBr	Reagent	10035-10-6	HBr	80.91	206.15[b]	186.15[b]
KOAc	Reagent	127-08-2	$C_2H_3KO_2$	98.14	–	565.15[b]
PyI	Intermediate	–	$C_8H_{10}INO$	263.08	–	–
KBr	By-product	7758-02-3	KBr	119.00	1708.15[b]	1003.15[b]
HOAc	By-product	64-19-7	$C_2H_4O_2$	60.05	391.15[b]	289.85[b]
HMS	Product	955369-56-9	$C_{17}H_{19}N_5O_2S$	357.43	838.75[a]	–
Cu(I)I	Catalyst	7681-65-4	CuI	190.45	1563.15[a]	878.15[a]
CyDMEDA	Ligand	67579-81-1	$C_8H_{18}N_2$	142.25	459.95[a]	283.38[a]
MeCN	Solvent	75-05-8	C_2H_3N	41.05	354.82[b]	228.15[b]

3. REACTION MECHANISM & KINETIC MODEL DEVELOPMENT

To develop a reaction mechanism which can accurately describe AZD1775 HMS synthesis, inspiration has been taken from a similar reaction already studied by Strieter

View Article Online
DOI: 10.1039/D5RE00082C

et al. [67]. Specifically, the copper-catalysed N-Arylation of Amides, since HMS synthesis occurs via Ullmann type coupling [68, 69]. It is important to note, however that we have adapted the reaction mechanism presented by these authors to allow several observations unique to HMS synthesis to be considered. These include:

1. The production of an aryl iodide compound (PyI), due to the presence of a side reaction involving PyBr (Figure 4).
2. The production of acetic acid (HOAc), which can hinder the progress of the reaction (Figure 4).
3. The presence of potassium acetate (KOAc), which may influence reaction rates (Figure 4).

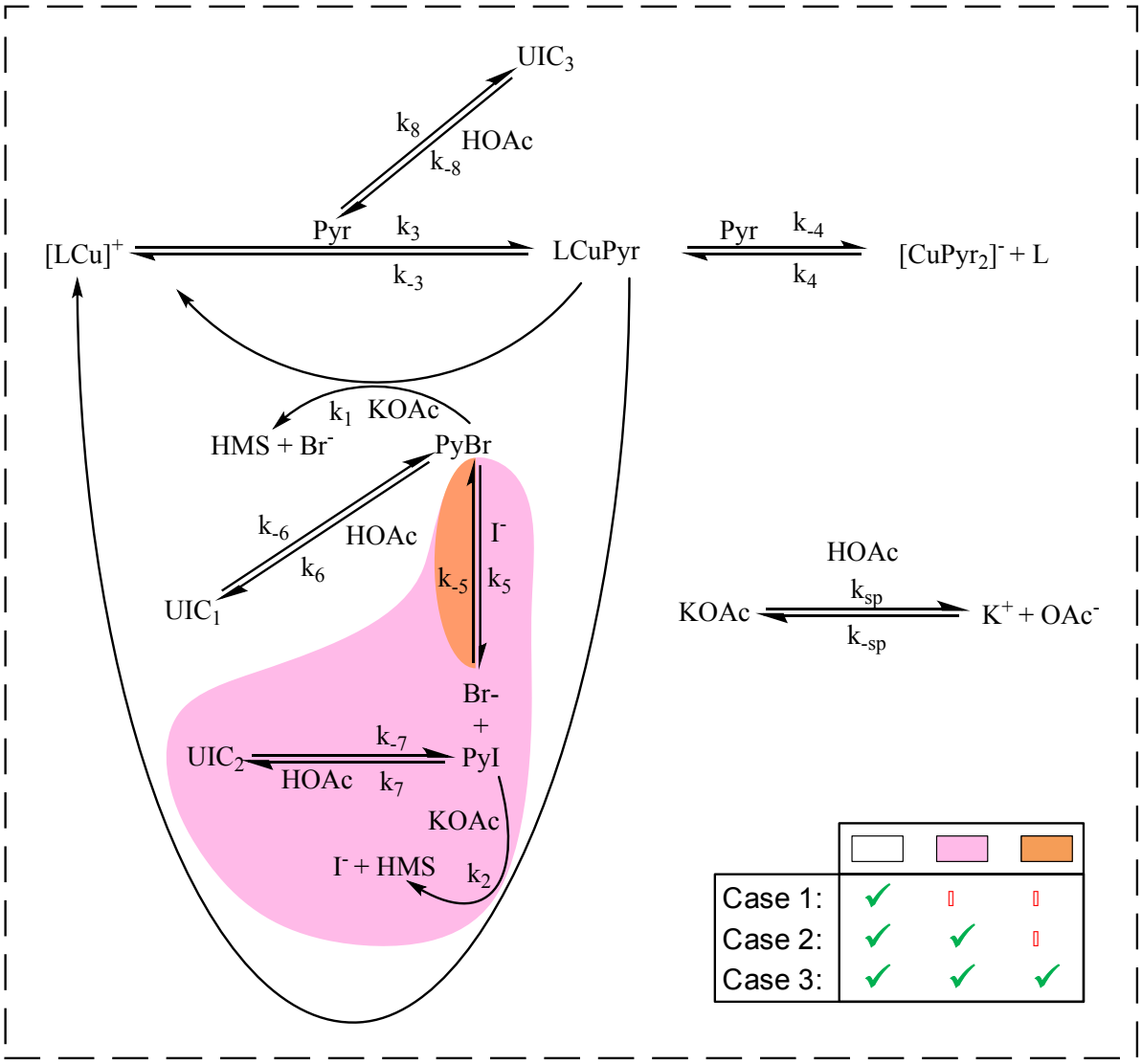

Figure 4. Proposed reaction mechanism for AZD1775 HMS synthesis. UIC_i represents as yet unidentified compounds formed due to the inhibitory action of HOAc.

Using this approach, we have defined three basic regimes under which different kinetic models can be developed to describe HMS synthesis (Figure 4). These are:

- Case 1: AZD1775 HMS Synthesis Disregarding PyI Production
- Case 2: AZD1775 HMS Synthesis Considering Irreversible PyI Production
- Case 3: AZD1775 HMS Synthesis Considering Reversible PyI Production

View Article Online
DOI: 10.1039/D5RE00082C

Each of these cases can be described using systems of differential algebraic equations (DAEs), as shown in Table 4. Where R_1 and R_2 respectively denote HMS synthesis from PyBr and PyI; whilst R_3 and R_4 denote the production and reversible consumption of PyI (Figure 4). However, to summarise their differences, we note that in case 1 the production of PyI from PyBr is completely ignored – allowing us to treat PyBr and PyI as a single pseudo aryl halide (PyHal). Meanwhile, in cases 2 and 3, we actively consider rate laws for PyI production via irreversible (Case 2) and reversible (Case 3) halide substitution reactions. Thereby, allowing PyBr and PyI to both react with Pyr independently to produce HMS.

Table 4. System of DAEs associated with each case developed.

Case 1	Case 2	Case 3
$\frac{d[Pyr]}{dt} = -R_1$	$\frac{d[Pyr]}{dt} = -R_1 - R_2$	$\frac{d[Pyr]}{dt} = -R_1 - R_2$
$\frac{d[PyrBr]}{dt} = -R_1$	$\frac{d[PyBr]}{dt} = -R_1 - R_3$	$\frac{d[PyBr]}{dt} = -R_1 - R_3 + R_4$
$\frac{d[KOAc]}{dt} = -2R_1$	$\frac{d[PyI]}{dt} = R_3 - R_2$	$\frac{d[PyI]}{dt} = R_3 - R_2 - R_4$
$\frac{d[HOAc]}{dt} = 2R_1$	$\frac{d[KOAc]}{dt} = -2R_1 - 2R_2$	$\frac{d[KOAc]}{dt} = -2R_1 - 2R_2$
$\frac{d[KBr]}{dt} = 2R_1$	$\frac{d[HOAc]}{dt} = 2R_1 + 2R_2$	$\frac{d[HOAc]}{dt} = 2R_1 + 2R_2$
$\frac{d[HMS]}{dt} = R_1$	$\frac{d[KBr]}{dt} = 2R_1 + 2R_2$	$\frac{d[KBr]}{dt} = 2R_1 + 2R_2$
	$\frac{d[HMS]}{dt} = R_1 + R_2$	$\frac{d[HMS]}{dt} = R_1 + R_2$

Within each of these cases, however, different rate laws may be used to describe:

1. The mechanism by which HMS synthesis occurs (whether from PyBr, PyI or the pseudo aryl halide PyHal defined)
2. The influence of HOAc on reaction rate
3. The impact of KOAc concentration on reaction rate
4. PyI production

Consequently, candidate rate laws for each of these aspects have been covered in Section 3.1 for each case.

3.1. Candidate Rate Laws for Cases 1-3

Full kinetic models developed for each case have been provided in the Supplementary Information (Case 1: Table S2, Case 2: Table S3, and Case 3: Table S4). However, the individual rate laws which have been used to make up each of these kinetic models have been provided in the following sections.

3.1.1. AZD1775 HMS Synthesis Disregarding PyI Production (Case 1)

The production of HMS occurs via Ullmann type coupling similar to the work of Strieter et al. [67]. Thus, assuming PyBr and PyI can be treated as a single compound (PyHal), HMS synthesis may be described using the rate law presented in Equations 1-2.

View Article Online
DOI: 10.1039/D5RE00082C

$$R_1 = k_1[LCuPyr][PyHal] \quad (1)$$

$$[LCuPyr] = \frac{K_3K_4[CuI]_0[L][Pyr]}{K_3[Pyr]^2 + K_4[L] + K_3K_4[Pyr][L]} \quad (2)$$

Atop of this, however, it has been postulated that potassium acetate (KOAc) may impact reaction rate. Thus, an alternative rate law for HMS synthesis has been defined in this work which accounts for this possibility, as shown in Equation 3.

$$R_1 = k_1[LCuPyr][PyHal]\left(K_{sp}[KOAc]\right)^{\alpha} \qquad \text{where: } \alpha \in [0, 1] \quad (3)$$

In addition to this, it has been suggested that HMS may be produced via a two-step Ullmann type coupling reaction (Figure 5). Hence, it is also possible that the reaction proceeds with 2nd order dependence on the ligated Pyrimidine compound (LCuPyr) [68, 69]; leading to the development of a second candidate rate law, as shown in Equation 4.

$$R_1 = k_1[LCuPyr]^2[PyHal]\left(K_{sp}[KOAc]\right)^{\alpha} \qquad \text{where: } \alpha \in [0, 1] \quad (4)$$

Alongside these considerations, however, it is also important to consider the possibility that acetic acid (HOAc) impacts the rate of reaction. Hence, reversible processes have been defined which temporarily take reactants off-cycle from the main reaction to model this effect (Equations 5-6).

$$[PyHal] = \frac{[PyHal]_{total}}{1 + [HOAc]K_6} \quad (5)$$

$$[Pyr] = \frac{[Pyr]_{total}}{1 + [HOAc]K_8} \quad (6)$$

It is important to note, however, that the nature of the compounds produced by these side processes (Equations 5-6) is unknown. Thus, we have simply represented them as UIC_1 and UIC_3 in this work (Figure 4).

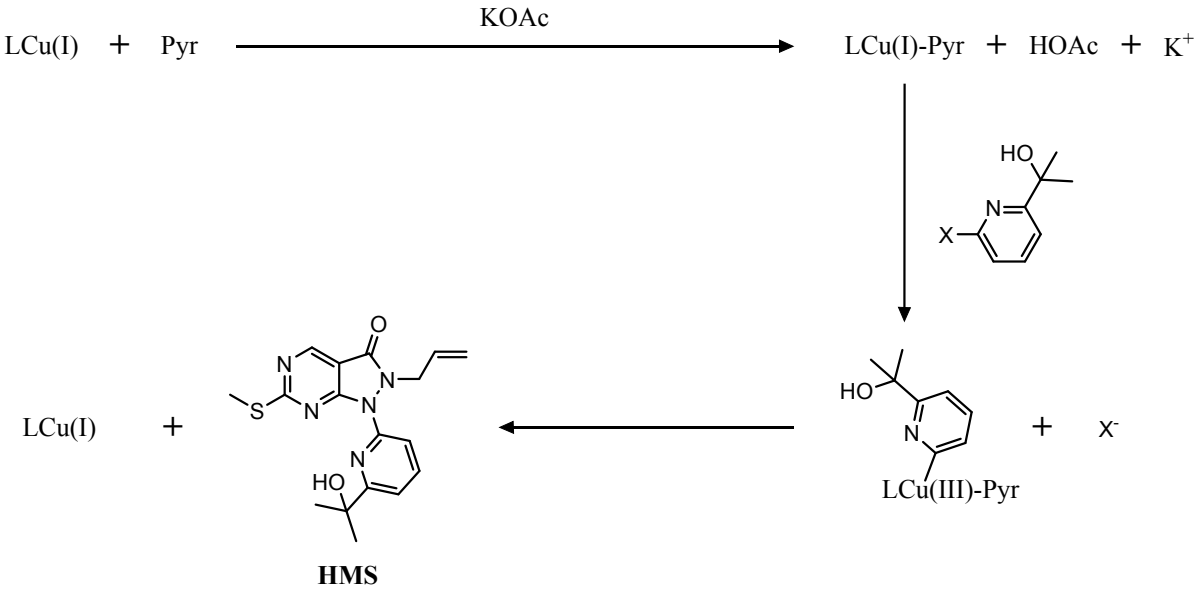

Figure 5. Ullmann type coupling [68, 69] expected during AZD1775 HMS formation.

View Article Online
DOI: 10.1039/D5RE00082C

Considering each of these options, it is clear that either Equation 3 or 4 could be used to describe HMS synthesis, by setting α to 0 or 1. Meanwhile, Equations 5 and 6 could be used to augment Equations 3 and 4 to account for the effects of HOAc. Consequently, a total of 16 kinetic models could be built for case 1 – full details of which can be found in the Supplementary Information (Table S2). In light of this, we name these models 1-16.

3.1.1.1. Calculating Ligand Concentration

To calculate concentration of the free-ligand (as is required for each model, according to Equation 2), we define its concentration in terms of observable species only. To do this, we note that the concentration of the catalyst and free-ligand may be defined in terms of the Cu-bound and ligated species as per Equations 7-8. Which, when combined and rearranged, afford Equation 9.

$$[L]_{total} = [L] + [LCu]^+ + [LCuPyr] \quad (7)$$

$$[CuI]_{total} = [CuI]_0 = [LCu]^+ + [LCuPyr] + [CuPyr_2]^- \quad (8)$$

$$[L] = [L]_{total} - [CuI]_0 + [CuPyr_2]^- \quad (9)$$

Following this, we use Figure 4 to define Equation 10; before combining it with Equations 2 and 9 to produce Equation 11 (after extensive algebraic rearrangement).

$$K_4 = \frac{[LCuPyr][Pyr]}{[CuPyr_2]^-[L]} \quad (10)$$

Equation 11 is a simple quadratic equation, solvable at each timestep for the reaction.

$$\begin{aligned}&(K_3K_4[Pyr] + K_4)[L]^2 \\ &+ \left(K_3[Pyr]^2 + K_3K_4[CuI]_0[Pyr] + K_4[CuI]_0 - K_4[L]_{total} - K_3K_4[Pyr][L]_{total}\right)[L] \\ &- K_3[Pyr]^2[L]_{total} = 0\end{aligned} \quad (11)$$

3.1.2. AZD1775 HMS Synthesis Considering Irreversible PyI Production (Case 2)

In case 2, HMS synthesis has been modelled assuming Ullman type coupling just as in case 1. Importantly, however, it also considers the production of PyI; assuming that it is produced irreversibly from PyBr. Consequently, HMS production for case 2 has been defined using Equations 12-13 to describe HMS synthesis from PyBr (Equation 12: one-step coupling, Equation 13: two-step coupling), whilst Equations 14-15 have been used to describe its production from PyI (Equation 14: one-step coupling, Equation 15: two-step coupling).

$$R_1 = k_1[LCuPyr][PyBr]\left(K_{sp}[KOAc]\right)^{\alpha} \quad \text{where: } \alpha \in [0, 1] \quad (12)$$

$$R_1 = k_1[LCuPyr]^2[PyBr]\left(K_{sp}[KOAc]\right)^{\alpha} \quad \text{where: } \alpha \in [0, 1] \quad (13)$$

$$R_2 = k_2[LCuPyr][PyI]\left(K_{sp}[KOAc]\right)^{\alpha} \quad \text{where: } \alpha \in [0, 1] \quad (14)$$

$$R_2 = k_2[LCuPyr]^2[PyI]\left(K_{sp}[KOAc]\right)^{\alpha} \quad \text{where: } \alpha \in [0, 1] \quad (15)$$

View Article Online
DOI: 10.1039/D5RE00082C

Following this logic, expressions (similar to Equations 5-6 from case 1) have been defined to describe the inhibitory effect of HOAc on PyBr, PyI and Pyr independently (Equations 16-18).

$$[PyBr] = \frac{[PyBr]_{total}}{1 + [HOAc]K_6} \quad (16)$$

$$[PyI] = \frac{[PyI]_{total}}{1 + [HOAc]K_7} \quad (17)$$

$$[Pyr] = \frac{[Pyr]_{total}}{1 + [HOAc]K_8} \quad (18)$$

In line with this, a variety of rate laws have been tested for the production of PyI from PyBr; all of which are reminiscent of those seen in other areas of chemistry where halogenic substitution takes place [70-79]. For example, it was noted that some studies [71-73] have found that halogenic substitution reactions involving pyridines follow second order rate laws which are first order in both the substrate and solvent. Meanwhile, it was found that a recent study conducted by Kundu et al. [74] looked at the reaction mechanisms underpinning ligand-assisted substitution reactions involving pyridines and their derivatives; concluding that such reactions proceed via 3rd order reactions (first order in catalyst; 2nd order in aryl halide substrate) [74]. Whereas other authors [70, 71] have suggested that such reactions proceed with rate laws of non-integer order (i.e., between 1 and 2). Consequently, two variable-order rate laws have been tested to allow each of these possibilities to be examined simultaneously; limiting the reaction order with respect to PyBr to between 1 and 2 (Equations 19-20). This simplified the problem, since it removed the need to explicitly quantify acetonitrile and copper (I) iodide concentrations; whilst leaving β to be set as an extra kinetic parameter to be estimated.

$$R_3 = k_5'[PyBr]^{\beta} \qquad \text{where: } k_5' = k_5[MeCN] \approx k_5[CuI] \quad (19)$$

$$R_3 = k_5[CuI]_0[PyBr]^{\beta} \quad (20)$$

This approach resulted in a total of 32 models for case 2 (named models 17-48), the full details of which can be found in the Supplementary Information (Table S3).

3.1.3. AZD1775 HMS Synthesis Considering Reversible PyI Production (Case 3)

In case 3, we retain Equation 2 from case 1 and Equations 12-18 from case 2 to describe the production of HMS from PyBr and PyI. However, we replace our treatment of PyI to consider its reversible production from PyBr. Specifically, via a reversible copper-catalysed Finkelstein reaction (Equations 21-22) [75-79].

$$R_3 = k_5[CuI]_0[PyBr][I^-] \qquad \text{where: } [I^-] \approx [I^-]_0 + [CuI]_0 - [PyI] \quad (21)$$

$$R_4 = k_{-5}[KBr][PyI] \quad (22)$$

This led to the development of 16 kinetic models for case 3, resulting in a total of 64 models across all three cases. Consequently, the kinetic models arising from case 4 have been named models 49-64. A full description of each model developed as part of case 3 can be found in the Supplementary Information (Table S4).

View Article Online
DOI: 10.1039/D5RE00082C

3.2. Rate Law Temperature Dependence

To capture the temperature dependence of each reaction step, Arrhenius and van't Hoff relationships have been included within each of the kinetic models devised (Equations 23-25).

$$k_n = k_{n,ref} e^{\frac{-E_{a,n}}{R}\left(\frac{1}{T}-\frac{1}{T_{ref}}\right)} \tag{23}$$

$$K_n = K_{n,ref} e^{\frac{-\Delta H_n^0}{R}\left(\frac{1}{T}-\frac{1}{T_{ref}}\right)} \tag{24}$$

$$K_n = \frac{k_n}{k_{-n}} \tag{25}$$

Likewise, the temperature dependence of the solubility product associated with KOAc in HOAc [80] has been estimated using the van't Hoff equation (Equations 26-27) [81] (Figure 6).

$$K_{sp} = x_{KOAc}^2 \tag{26}$$

$$\ln(x_{KOAc}) = -\frac{\Delta H_d^0}{RT} + \frac{\Delta S_d^0}{R} \tag{27}$$

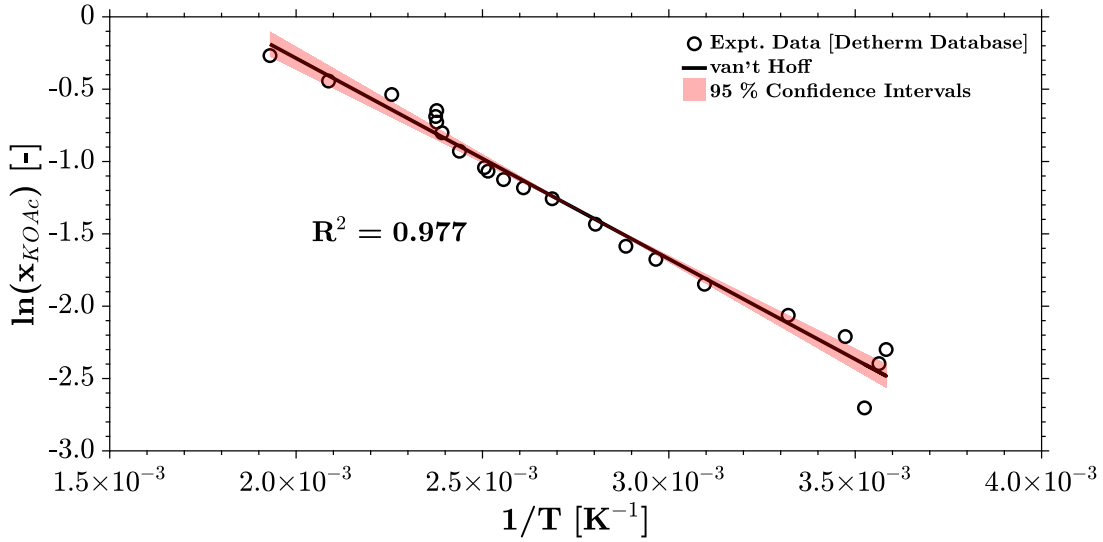

Figure 6. Temperature dependent KOAc solubility in HOAc (data from [80]).

4. PARAMETER ESTIMATION & MODEL DISCRIMINATION

Parameter estimation and model discrimination techniques have been used alongside one another to identify the most appropriate kinetic model for HMS synthesis from the 64 models developed in Section 3. Consequently, the procedure used to achieve this has been summarised in Figure 7, while Sections 4.1 and 4.2 have been provided below to offer deeper explanations of each of the blocks represented by this diagram.

It is important to note, however, that each case (and model) has been studied independently using multistart nonlinear programming (NLP). Hence, any parameter estimation efforts have been conducted for each model individually before using model discrimination techniques to analyse the results from each of these studies.

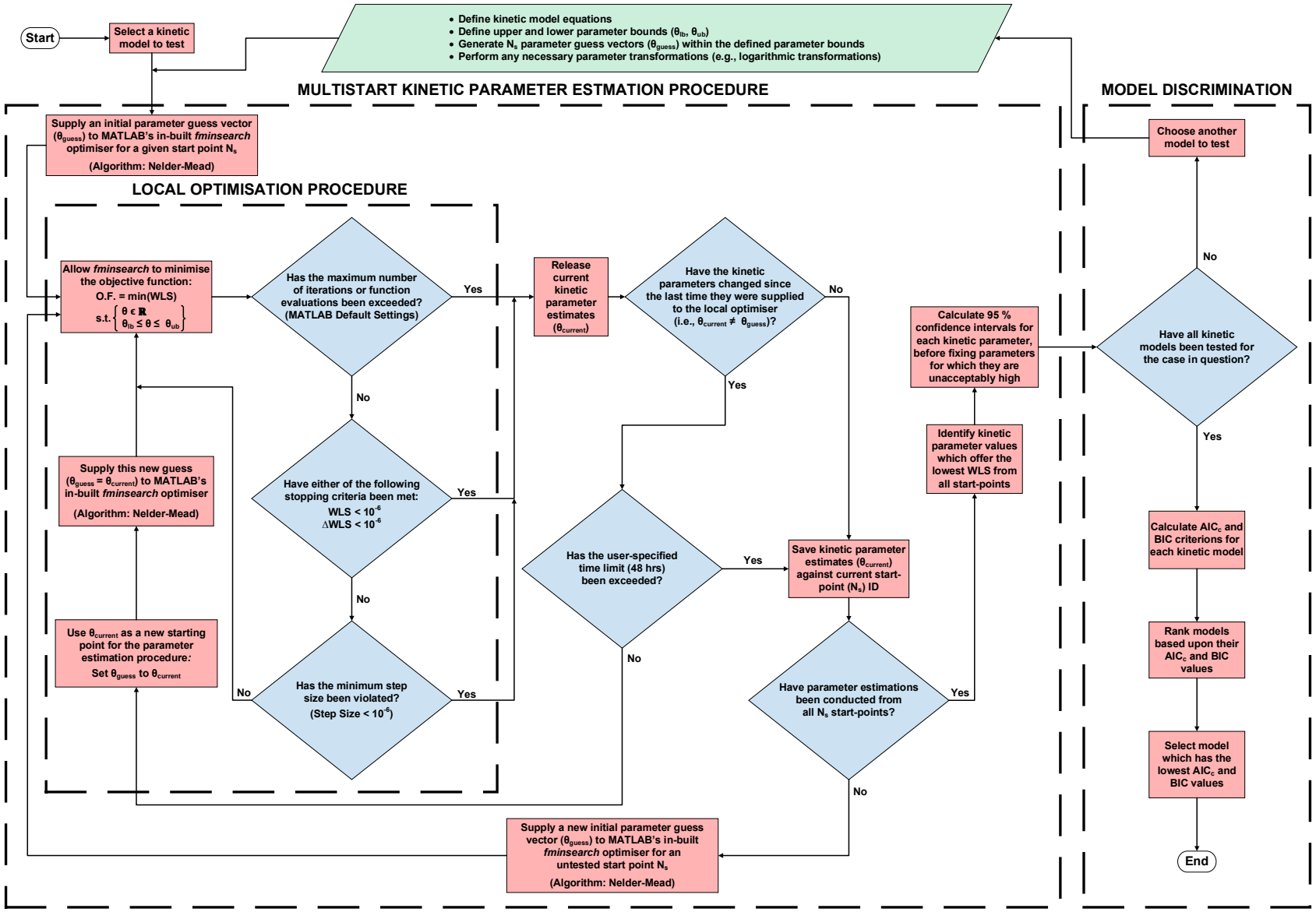

Figure 7. Procedure for kinetic parameter estimation and reaction model discrimination.

View Article Online
DOI: 10.1039/D5RE00082C

4.1. Kinetic Parameter Estimation Methodology

The parameter estimation problem has been formulated as a multistart constrained optimisation problem for each model, using the objective function described in Equations 28-33.

$$\min f(\boldsymbol{\theta}) \tag{28}$$

$$s.t. \begin{cases} f(\boldsymbol{\theta}) = WLS & (29) \\ \boldsymbol{\theta} = \left[k_{n,ref}, E_{a,n}, \Delta H_n^0, K_{n,ref}, \Delta H_d^0, \Delta S_d^0, \beta\right] & (30) \\ \boldsymbol{\theta_{lb}} \leq \boldsymbol{\theta} \leq \boldsymbol{\theta_{ub}} & (31) \\ \boldsymbol{\theta} \in \mathbb{R} & (32) \end{cases}$$

$$WLS = \frac{1}{2}\sum_{i=1}^{N_{species}} \sum_{j=1}^{N_{data}} W_i \left(C_{i,j}^{expt} - C_{i,j}^{model}\right)^2 \tag{33}$$

Using this approach, parameter estimations could be initialised from 1000 different start-points for each model, using 1000 different random guess-vectors containing different parameter values within the specified bounds (Table 5). Noting that (in order to avoid divergence) any parameter values calculated during these estimations which result in non-numeric, infinite or imaginary objective function values must be rejected – forcing the optimisation algorithm to alter the space in which it is searching.

Interested readers can find an explanation of the code structure used to achieve this in Section 4.1.1 below. However, in short, the kinetic parameters and reaction orders required by each model have been estimated using an in-house parameter estimation code written in MATLAB® (Figure 7). Specifically, one which places MATLAB's *fminsearch* tool (which separately employs the Nelder-Mead algorithm) at the centre of a *while* loop, with the aim of iteratively minimising the sum of weighted least squares (Equation 33) associated with each model. Importantly, setting any weights (W_i) to the reciprocal of the square uncertainties of the experimental measurements; whilst also placing user-specified bounds on each of the parameters to be estimated (Table 5).

To enable this approach, it has been stipulated that any kinetic rate constants appearing in the kinetic models tested can take on values of between 0-6×10^{11}; since liquid phase bimolecular reactions are thought not exceed rates of 6×10^{11} M^{-1} min^{-1} [82-86]. Likewise, it has been specified that any activation energies, $E_{a,n}$, must have values of between 1-150 kJ mol^{-1} to align with expectations from classical organic synthesis reactions [87]. Meanwhile, it has been acknowledged that standard reaction enthalpies, ΔH_n^0, for organic reactions are between -1000 and 1000 kJ mol^{-1}; whilst their equilibrium constants, K_n, have values of 0.01-100 whenever equilibrium concentrations are measurable [88]. Whereas, any reaction orders, β, must be bounded between 1 and 2 (for the reasons previously mentioned in Section 3); leaving KOAc dissolution properties (ΔH_d^0 and ΔS_d^0) to be set limits equal to their 95 % confidence intervals (as shown in Figure 6).

Given the range of each of these bounds, the search space for each problem has been reduced by taking natural logarithm transforms of parameters $k_{ref,n}$, $E_{a,n}$ and K_{ref} – a practice that has been advocated by serval authors [89, 90]. This approach was not possible when dealing with ΔH_n^0 parameters, however, since this would have resulted

View Article Online
DOI: 10.1039/D5RE00082C

in imaginary solutions which had no physical meaning. Meanwhile, it was not worthwhile when estimating β parameters given the small range of values considered.

Table 5. Parameter bounds.

	$k_{n,ref}$ [various]	$K_{n,ref}$ [various]	$E_{a,n}$ [kJ mol^{-1}]	ΔH_n^0 [kJ mol^{-1}]	ΔH_d^0 [kJ mol^{-1}]	ΔS_d^0 [kJ mol^{-1} K^{-1}]	β [–]
Lower Bound (θ_{lb})	10^{-10}	0.01	1	-1000	10.702	0.0184	1
Upper Bound (θ_{ub})	6×10^{11}	100	150	1000	12.365	0.0230	2

4.1.1. Code Structure

Parameter estimation has been carried out for each kinetic model independently (i.e., models 1-64) using a parameter estimation code based on two simple concepts:

1) *Local Optimisation*: MATLAB's *fminsearch* tool (Algorithm: Nelder-Mead) is used to minimise the objective function of each model (Equations 28-33) by varying the value of their model parameters ($\boldsymbol{\theta}$) within their specified bounds. Moreover, it continues to do so until one of the following criteria is met:
   a) The maximum number of iterations or objective function evaluations is exceeded (MATLAB default settings used).
   b) The objective function is less than 10^{-6}, or cannot be improved upon by more than 10^{-6}.
   c) The minimum step size (10^{-6}) has been violated.

   Once one of these criteria is met, *fminsearch* releases any parameter estimates held ($\boldsymbol{\theta_{current}}$) before checking to see if one of the following criteria has also been satisfied:
   d) The kinetic parameters have not changed compared to the values last supplied to the optimiser.
   e) The user-specified maximum allowable time for estimations (48 hrs) has been exceeded.

   If one of (d) or (e) has been satisfied, then the current parameter estimates ($\boldsymbol{\theta_{current}}$) are saved against their associated start-point identification number (N_s) for later analysis. However, if neither of these criteria have been achieved, then the outputted parameter estimates ($\boldsymbol{\theta_{current}}$) are re-supplied to *fminsearch* as a new initial guess. This serves to enhance convergence by repeating step 1 until (a)-(c) and one of (d) or (e) are satisfied (Figure 7).

2) *Multistart Problem Initialisation*: To improve estimations, step 1 is repeated using 1000 different initial guesses ($\boldsymbol{\theta_{guess}}$) before selecting the set of parameters returned which afford the lowest objective function value. Following this, 95 % confidence intervals are calculated for the selected parameter set, noting that parameters which give unacceptably high confidence intervals (i.e., greater than 15 % [23, 24, 48, 56]) should be fixed [39, 91] (Figure 7).

In light of this, it is possible to run the parameter estimation code used in series or parallel – depending on the computing facilities available to the user. However, it should be noted that running estimations in parallel (e.g., by splitting jobs across multiple computing cores) will invariably provide faster results, since computational cost scales linearly with the number of start-points used.

View Article Online
DOI: 10.1039/D5RE00082C

4.2. Model Discrimination

Following parameter estimation, the Akaike Information Criterion (AIC_c) has been used to rank each model based on its: (i) simplicity, and (ii) ability to match experimental observations [23, 56] (Equation 34). Consequently, models with lower AIC_c values have been favoured in this work, since this indicates that a model can accurately represent experimental findings whilst avoiding the use of unnecessary terms – preventing overfitting and over-parameterisation as a result [23].

$$AIC_c = N_{obs} \ln\left(\frac{WLS}{N_{obs}}\right) + 2N_{param} + \frac{2N_{param}\left(N_{param}+1\right)}{N_{obs} - N_{param} - 1} \tag{34}$$

Alongside this, relative Akaike likelihoods (Equations 35-36) have been used to determine the probability that the model found to have the lowest AIC_c for a given case is indeed better than all other model candidates available for that case. Meanwhile, evidence ratios (Equation 37) and normalized probabilities (Equation 38) have been calculated for each model to assess the likelihood that the selected model is better than the next-best model (i.e., the probability that model i is suitable when compared with model j) [58, 60, 92, 93].

$$w_{i,AIC_c} = \frac{\exp\left(-\frac{1}{2}\Delta(AIC_c)_i\right)}{\sum_{j=1}^{N_{mdl}} \exp\left(-\frac{1}{2}\Delta(AIC_c)_j\right)} \tag{35}$$

$$\Delta(AIC_c)_i = (AIC_c)_i - (AIC_c)_{min} \tag{36}$$

$$(ER)_{AIC_c} = \frac{w_{i,AIC_c}}{w_{j,AIC_c}} \tag{37}$$

$$(NP)_{AIC_c} = \frac{w_{i,AIC_c}}{w_{i,AIC_c} + w_{j,AIC_c}} \tag{38}$$

It is important to note, however, that the Bayesian Information Criterion (BIC) has also been estimated for each model (Equation 39) to support these efforts; calculating normalised probabilities in the same manner as for AIC_c. Hence, models with lower BIC values also represent more promising models; with BIC penalising model complexity more harshly than AIC_c [59].

$$BIC = N_{obs} \ln\left(\frac{WLS}{N_{obs}}\right) + N_{param} \ln(N_{obs}) \tag{39}$$

5. RESULTS

As discussed in Section 3, three distinct cases were considered when developing kinetic models to describe HMS synthesis:

- Case 1: AZD1775 HMS Synthesis Disregarding PyI Production
- Case 2: AZD1775 HMS Synthesis Considering Irreversible PyI Production
- Case 3: AZD1775 HMS Synthesis Considering Reversible PyI Production

Consequently, Figure 8 has been used to provide an overview of the AIC_c and BIC values calculated for each model on a case-by-case basis; ultimately providing a ranking for each model within these three cases.

View Article Online
DOI: 10.1039/D5RE00082C

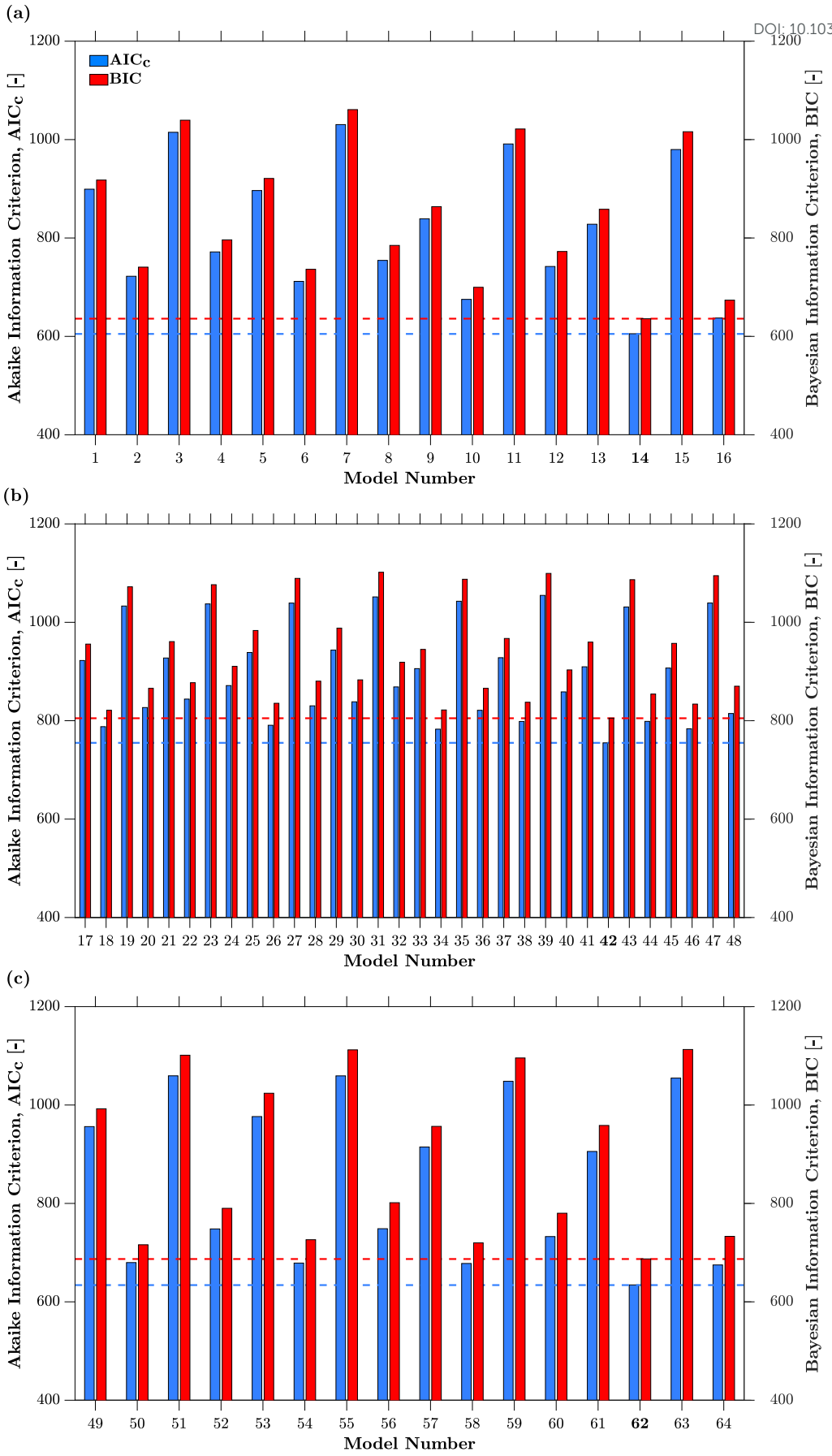

Figure 8. $\boldsymbol{AIC_c}$ and $\boldsymbol{BIC}$ values: (a) Case 1 (no Pyl production); (b) Case 2 (irreversible Pyl production); and (c) Case 3 (reversible Pyl production) reaction model networks.

View Article Online
DOI: 10.1039/D5RE00082C

Considering these results, models 14, 42 and 62 can be determined as the most promising model candidates from cases 1, 2 and 3, respectively. In fact, the normalised AIC_c and BIC probabilities both sit at 1.0 for each of these models when compared with the next-best model from their respective cases. Alongside this, however, it was also observed that of the models used to consider Pyl production (i.e., those from cases 2 and 3), model 62 outperformed model 42 by a significant margin. In fact, model 62 exhibited WLS, AIC_c and BIC values 50.10, 16.03 and 14.66 % lower than model 42. Hence, model 42 has been rejected, allowing model 62 to be accepted ahead of all other models developed to handle Pyl production.

In light of these realisations, the reaction profiles predicted by models 14 and 62 have been compared with experimental data in Figure 9 and Figure 10, respectively. Meanwhile, final kinetic parameters associated these models have been provided in Table 6. It should be noted, however, that both models 14 and 62 experience looser fits for experiment "l" than for the rest of the experiments. This is likely due to undercalculation of HMS concentrations for this experiment (possibly caused by non-uniform mixing), since less HMS was produced than Pyr consumed in this experiment yet no other species were observed during HPLC measurements. The use of WLS regression when conducting this work was able to successfully mitigate the effects of this, however. Especially since similar percentage uncertainties are associated with each experimental data point measured; leading to larger absolute experimental uncertainties for species with higher concentrations (such as HMS in experiment "l").

Table 6. Kinetic parameters (estimated and fixed) for models 14 and 62.

	Model 14	**Model 62**
$\boldsymbol{k_{1,ref}}$ [M^{-2} min^{-1}]	131.339 (± 1.140 %)	852.151 (± 2.164 %)
$\boldsymbol{k_{2,ref}}$ [M^{-2} min^{-1}]	–	12273.399 (fixed)
$\boldsymbol{k_{5,ref}}$ [M^{-2} min^{-1}]	–	1.482 (± 0.014 %)
$\boldsymbol{K_{3,ref}}$ [M]	99.993 (± 0.011 %)	8.004 (± 0.086 %)
$\boldsymbol{K_{4,ref}}$ [–]	0.166 (± 0.148 %)	0.052 (± 0.063 %)
$\boldsymbol{K_{5,ref}}$ [M^{-1}]	–	9.284 (fixed)
$\boldsymbol{K_{6,ref}}$ [M]	4.112 (± 10.168 %)	0.549 (± 2.408 %)
$\boldsymbol{K_{7,ref}}$ [M]	–	6.977 (fixed)
$\boldsymbol{K_{8,ref}}$ [M]	8.057 (± 6.120 %)	2.296 (± 5.839 %)
$\boldsymbol{E_{a,1}}$ [kJ mol^{-1}]	146.134 (± 7.539 %)	31.272 (± 9.268 %)
$\boldsymbol{E_{a,2}}$ [kJ mol^{-1}]	–	1.045 (fixed)
$\boldsymbol{E_{a,5}}$ [kJ mol^{-1}]	–	60.497 (± 3.047 %)
$\Delta\boldsymbol{H_3^0}$ [kJ mol^{-1}]	200.464 (± 1.030 %)	-309.601 (± 1.146 %)
$\Delta\boldsymbol{H_4^0}$ [kJ mol^{-1}]	0.825 (± 1.045 %)	9.908 (± 2.465 %)
$\Delta\boldsymbol{H_5^0}$ [kJ mol^{-1}]	–	253.532 (fixed)
$\Delta\boldsymbol{H_6^0}$ [kJ mol^{-1}]	404.302 (± 6.580 %)	-515.590 (± 3.211 %)
$\Delta\boldsymbol{H_7^0}$ [kJ mol^{-1}]	–	-584.127 (± 10.448 %)
$\Delta\boldsymbol{H_8^0}$ [kJ mol^{-1}]	102.235 (fixed)	-217.411 (± 8.344 %)

From these findings, it can be observed that both of the final models selected share all of the same model aspects as one another – aside from their treatment of Pyl production (c.f. model structures in Table S2 and Table S4 within the Supplementary Information). Thus, it may be concluded that each of the aspects accounted for by these models must play a key role in the synthesis of HMS. For example, since the production of HMS from aryl halides and Pyr is second order in $LCuPyr$ concentration

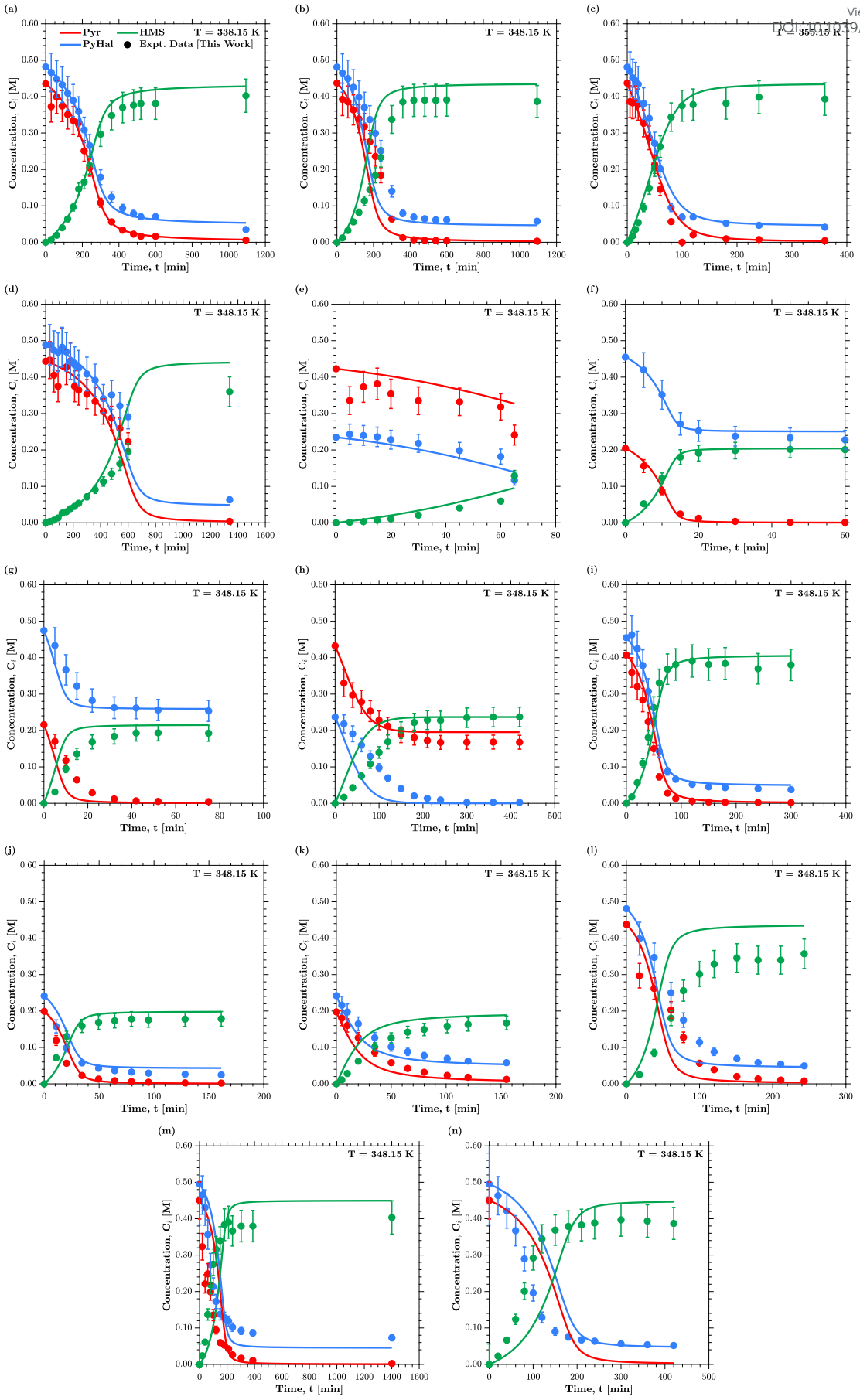

Figure 9. Kinetic model predictions versus experimental data (model 14).

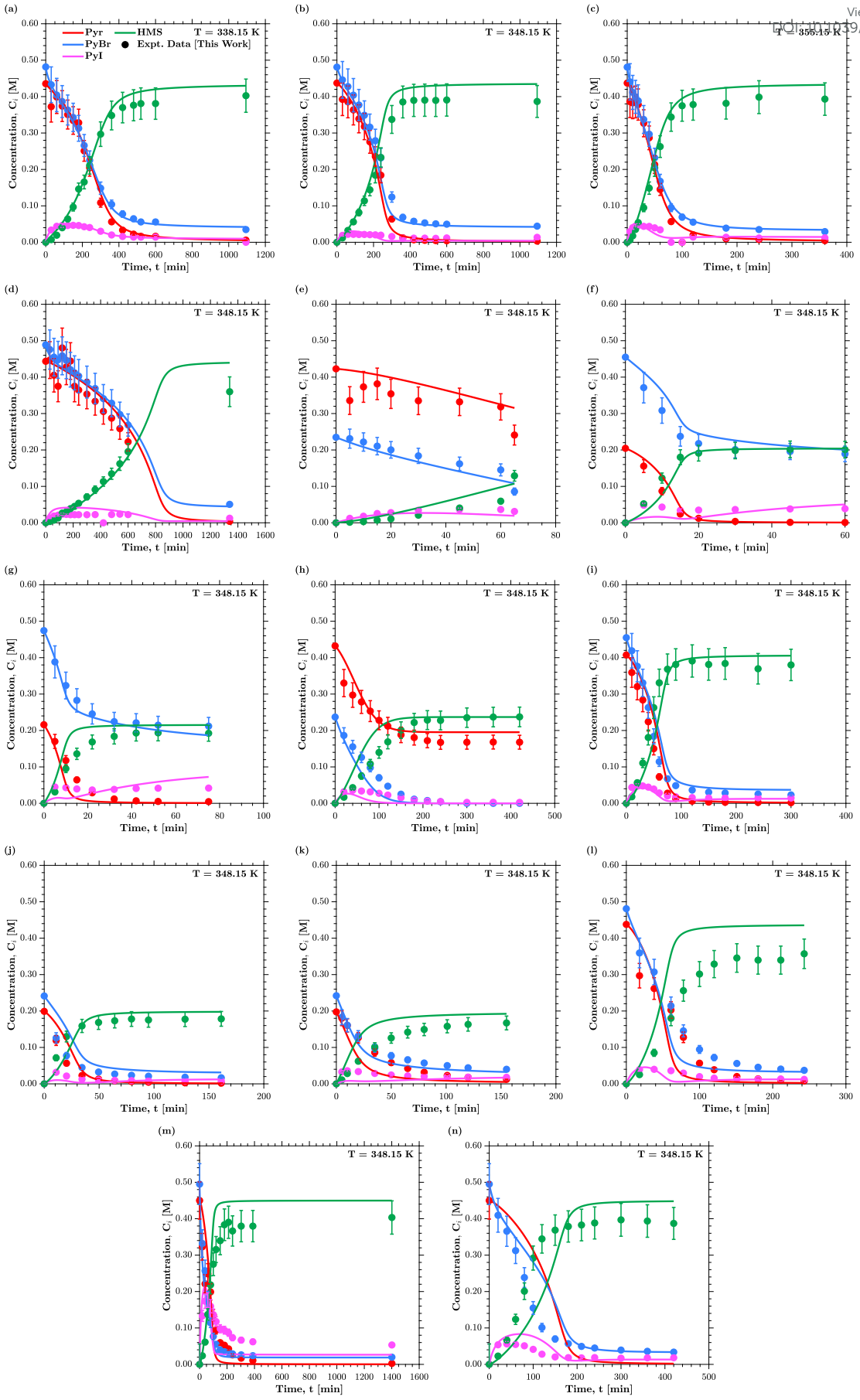

Figure 10. Kinetic model predictions versus experimental data (model 62).

View Article Online
DOI: 10.1039/D5RE00082C

for both models, it is likely that 2-step Ullmann coupling (Figure 5) occurs in place of a 1-step mechanism. Meanwhile, any aspects ignored by these models (e.g., KOAc concentration dependence) are unlikely to have a notable effect on the reaction.

In line with this, it can also be concluded that PyI is most likely produced via a copper-catalysed Finkelstein reaction, since the kinetic models built using this assumption (i.e., those in case 3) often outperformed their equivalent counterparts (i.e., those in case 2). However, further experimentation focused on analysing the production of PyI would be required to fully confirm this theory. Likewise, given the fact that both models selected consider inhibitory effects brought about by the presence of HOAc, it is possible that the presence of this acid does indeed inhibit the action of Pyr, PyBr and PyI. The exact mechanism by which this inhibition occurs remains unclear (as discussed in Section 3, Figure 4), however; so future work should attempt to establish the true mechanism by which this HOAc inhibition occurs. Though current thinking is that the presence of HOAc may create a buffer system which impacts the deprotonation of pyrimidine and slows down the oxidative addition of the aryl halides as a result (Figure 5).

6. DISCUSSION & CONCLUSIONS

The reaction mechanism proposed within this work (Figure 4) successfully captured key aspects of AZD1775 HMS synthesis; allowing three broad types of kinetic model to be developed and tested. Specifically, those which modelled HMS synthesis by disregarding PyI production entirely (Case 1: Models 1-16) as well as those which considered its irreversible (Case 2: Models 17-48) and reversible (Case 3: Models 49-64) production. From this, a total of 64 candidate kinetic models could be developed to describe the copper-catalysed, and ligand-assisted, synthesis of HMS. However, candidates 14 and 62 showed the most promising results by some margin – exhibiting low objective function values and favourable AIC_c and BIC metrics following their successful parameterisation. As a consequence of this, it has been suggested by the authors that manufacturing facilities and research groups should use model 14 to model HMS synthesis if PyI production does not need to be explicitly quantified – since this model has a far simpler structure and reduced parameter set. While model 62 should be employed if one wishes to track PyI production more closely.

A critical remark is that the parameter estimation code and model development pursued herein does not guarantee uniqueness. Consequently, alternative models may yield comparable results to those achieved here, but they would also need be far more complex than those presented. Accordingly, future studies should focus on using the kinetic models offered here to identify optimal reaction conditions for HMS synthesis; manipulating process variables such as temperature, reaction time and initial reagent concentrations to maximise product yield whilst minimising side product generation. Furthermore, future parameter estimation studies can also incorporate parameter identifiability and estimability analyses [94, 95] in the respective workflows. Bootstrapping methods can also be incorporated into this workflow, for codes which will be addressing the study of scenarios under limited experimental data availability.

View Article Online
DOI: 10.1039/D5RE00082C

AUTHOR INFORMATION

Corresponding Author

*E-mail: D.Gerogiorgis@ed.ac.uk, phone: +44 131 6517072

ORCID

Matthew Blair https://orcid.org/0000-0001-9233-2173
Dimitrios I. Gerogiorgis: https://orcid.org/0000-0002-2210-6784

DECLARATION OF INTERESTS

The authors report no conflict of interest, financial or otherwise.

ACKNOWLEDGMENTS

This work has made use of resources provided by the Edinburgh Compute and Data Facility (ECDF) (http://www.ecdf.ed.ac.uk/). M. Blair acknowledges the financial support provided by AstraZeneca UK Limited and the Engineering and Physical Sciences Research Council (EPSRC) under the Industrial CASE Studentship scheme. The authors would also like to thank Dr Martin Jones for their help in organising and planning this studentship. The data cited and tabulated within this work is sufficient for the reproduction of all results.

NOMENCLATURE & ACRONYMS

Latin Letters

$C_{i,j}^{expt}$	Experimental concentration of species i at datapoint j [M]
$C_{i,j}^{model}$	Modelled concentration of species i at datapoint j [M]
$E_{a,n}$	Activation energy associated with forward reaction n [kJ mol^{-1}]
$f(\boldsymbol{\theta})$	Temperature dependent fitting objective function [–]
ΔH_d^0	Standard enthalpy of dissolution for KOAc in HOAc [kJ mol^{-1}]
ΔH_n^0	Standard reaction enthalpy with reaction n [kJ mol^{-1}]
$[i]$	Molar concentration of component i [M]
$[i]_0$	Initial molar concentration of component i [M]
k_n	Kinetic rate constant associated with forward reaction n [various]
$k_{n,ref}$	Pre-exponential reference constant for forward reaction n [various]
k_{-n}	Kinetic rate constant associated with reverse reaction n [various]
K_n	Equilibrium rate constant associated with reaction n [various]
K_{sp}	Solubility product [M^2]
M	Molecular weight [g mol^{-1}]
N_{data}	Number of experimental data points [–]
N_{mdl}	Number of models tested [–]
N_{obs}	Number of experimental observations (i.e, time-points) [–]
N_{param}	Number of parameters [–]
N_s	Number of start-points [–]
$N_{species}$	Number of species [–]

View Article Online
DOI: 10.1039/D5RE00082C

R	Universal gas constant [J mol^{-1} K^{-1}]
R_j	Reaction rate j [mol L^{-1} min^{-1}]
$\mathbb{R}$	Real numbers [–]
ΔS_d^0	Standard entropy of dissolution for KOAc in HOAc [kJ mol^{-1} K^{-1}]
t	Reaction time [min]
T	Reaction temperature [K]
T_{bp}	Boiling point temperature [K]
T_{mp}	Melting point temperature [K]
T_{ref}	Reference temperature [K]
w_{i,AIC_c}	Normalised relative Akaike likelihoods [–]
W_i	Objective function weight associated with measurement i [M^{-2}]
x_{KOAc}	Solubility of KOAc In HOAc at a given temperature [mol mol^{-1}]

Greek Letters

α	Binary decision variable [–]
β	Unknown rate order [–]
$\boldsymbol{\theta}$	Parameter vector [various]
$\boldsymbol{\theta_{current}}$	Parameter vector outputted at interim points during estimations [various]
$\boldsymbol{\theta_{guess}}$	Initial parameter vector guess for a given start-point [various]
$\boldsymbol{\theta_{lb}}$	Parameter vector lower bounds [various]
$\boldsymbol{\theta_{ub}}$	Parameter vector upper bounds [various]

Acronyms

AIC_c	Corrected Akaike's Information Criterion [–]
$(AIC_c)_i$	Corrected Akaike Information Criterion of model i [–]
$(AIC_c)_{min}$	Minimum Corrected Akaike Information Criterion obtained [–]
$\Delta(AIC_c)_i$	Corrected Akaike Differences of model i [–]
BIC	Bayesian Information Criterion [–]
$(ER)_{AIC_c}$	Corrected Akaike Evidence Ratios [–]
$(NP)_{AIC_c}$	Corrected Akaike Normalized Probabilities [–]
WLS	Weighted least squares [–]

REFERENCES

1. Prasad, V., De Jesus, K., and Mailankody, S., *The high price of anticancer drugs: origins, implications, barriers, solutions.* Nat Rev Clin Oncol, 2017. **14**(6): 381.
2. Jönsson, B., Hofmarcher, T., Lindgren, P., and Wilking, N., *The cost and burden of cancer in the European Union 1995–2014.* European Journal of Cancer, 2016. **66**: 162.
3. Hofmarcher, T., Lindgren, P., Wilking, N., and Jönsson, B., *The cost of cancer in Europe 2018.* European Journal of Cancer, 2020. **129**: 41.
4. Dyba, T., Randi, G., Bray, F., et al., *The European cancer burden in 2020: Incidence and mortality estimates for 40 countries and 25 major cancers.* European Journal of Cancer, 2021. **157**: 308.
5. Cancer Research UK. *Cancer Statistics for the UK*. [cited 2023 23rd March]; Available from: https://www.cancerresearchuk.org/health-professional/cancer-statistics-for-the-uk.
6. Siegel, R.L., Miller, K.D., Fuchs, H.E., and Jemal, A., *Cancer Statistics, 2021.* CA Cancer J Clin, 2021. **71**(1): 7.
7. Cancer Research UK. *Worlwide cancer statistics*. [cited 2023 25th May]; Available from: https://www.cancerresearchuk.org/health-professional/cancer-statistics/worldwide-cancer#heading-Zero.

8. Diab, S. and Gerogiorgis, D.I., *Process Modeling, Simulation, and Technoeconomic Evaluation of Separation Solvents for the Continuous Pharmaceutical Manufacturing (CPM) of Diphenhydramine.* Organic Process Research & Development, 2017. **21**(7): 924.
9. Diab, S. and Gerogiorgis, D.I., *Process modelling, simulation and technoeconomic evaluation of crystallisation antisolvents for the continuous pharmaceutical manufacturing of rufinamide.* Computers & Chemical Engineering, 2018. **111**: 102.
10. Diab, S. and Gerogiorgis, D.I., *Process modelling, simulation and technoeconomic optimisation for continuous pharmaceutical manufacturing of (S)-warfarin*, in *Computer Aided Chemical Engineering*, A. Friedl, et al., Editors. 2018, Elsevier, p. 1643.
11. Diab, S., McQuade, D.T., Gupton, B.F., and Gerogiorgis, D.I., *Process Design and Optimization for the Continuous Manufacturing of Nevirapine, an Active Pharmaceutical Ingredient for HIV Treatment.* Organic Process Research & Development, 2019. **23**(3): 320.
12. Diab, S., Mytis, N., Boudouvis, A.G., and Gerogiorgis, D.I., *Process modelling, design and technoeconomic Liquid–Liquid Extraction (LLE) optimisation for comparative evaluation of batch vs. continuous pharmaceutical manufacturing of atropine.* Computers & Chemical Engineering, 2019. **124**: 28.
13. Watson, O.L., Jonuzaj, S., McGinty, J., et al., *Computer Aided Design of Solvent Blends for Hybrid Cooling and Antisolvent Crystallization of Active Pharmaceutical Ingredients.* Organic Process Research & Development, 2021. **25**(5): 1123.
14. Jolliffe, H.G. and Gerogiorgis, D.I., *Plantwide design and economic evaluation of two Continuous Pharmaceutical Manufacturing (CPM) cases: Ibuprofen and artemisinin.* Computers & Chemical Engineering, 2016. **91**: 269.
15. Jolliffe, H.G. and Gerogiorgis, D.I., *Technoeconomic Optimization of a Conceptual Flowsheet for Continuous Separation of an Analgaesic Active Pharmaceutical Ingredient (API).* Industrial & Engineering Chemistry Research, 2017. **56**(15): 4357.
16. McDonald, M.A., Marshall, G.D., Bommarius, A.S., et al., *Crystallization Kinetics of Cephalexin Monohydrate in the Presence of Cephalexin Precursors.* Crystal Growth & Design, 2019. **19**(9): 5065.
17. Cuthbertson, A.B., Rodman, A.D., Diab, S., and Gerogiorgis, D.I., *Dynamic Modelling and Optimisation of the Batch Enzymatic Synthesis of Amoxicillin.* Processes, 2019. **7**(6): 318.
18. Diab, S., Raiyat, M., and Gerogiorgis, D.I., *Flow synthesis kinetics for lomustine, an anti-cancer active pharmaceutical ingredient.* Reaction Chemistry & Engineering, 2021. **6**(10): 1819.
19. Hone, C.A., Boyd, A., O'Kearney-McMullan, A., et al., *Definitive screening designs for multistep kinetic models in flow.* Reaction Chemistry & Engineering, 2019. **4**(9): 1565.
20. Içten, E., Maloney, A.J., Beaver, M.G., et al., *A Virtual Plant for Integrated Continuous Manufacturing of a Carfilzomib Drug Substance Intermediate, Part 1: CDI-Promoted Amide Bond Formation.* Organic Process Research & Development, 2020. **24**(10): 1861.
21. Cole, K.P., Campbell, B.M., Forst, M.B., et al., *An Automated Intermittent Flow Approach to Continuous Suzuki Coupling.* Organic Process Research & Development, 2016. **20**(4): 820.
22. Grom, M., Stavber, G., Drnovšek, P., and Likozar, B., *Modelling chemical kinetics of a complex reaction network of active pharmaceutical ingredient (API) synthesis with process optimization for benzazepine heterocyclic compound.* Chemical Engineering Journal, 2016. **283**: 703.
23. Taylor, C.J., Booth, M., Manson, J.A., et al., *Rapid, automated determination of reaction models and kinetic parameters.* Chemical Engineering Journal, 2021. **413**: 127017.
24. Schenk, C., Short, M., Rodriguez, J.S., et al., *Introducing KIPET: A novel open-source software package for kinetic parameter estimation from experimental datasets including spectra.* Computers & Chemical Engineering, 2020. **134**: 106716.

25. Jolliffe, H.G. and Gerogiorgis, D.I., *Process modelling and simulation for continuous pharmaceutical manufacturing of ibuprofen.* Chemical Engineering Research and Design, 2015. **97**: 175.
26. Echtermeyer, A., Amar, Y., Zakrzewski, J., and Lapkin, A., *Self-optimisation and model-based design of experiments for developing a C–H activation flow process.* Beilstein Journal of Organic Chemistry, 2017. **13**: 150.
27. Aroh, K.C. and Jensen, K.F., *Efficient kinetic experiments in continuous flow microreactors.* Reaction Chemistry & Engineering, 2018. **3**(1): 94.
28. Frederick, M.O., Pietz, M.A., Kjell, D.P., et al., *Development of a Leuckart–Wallach Reaction in Flow for the Synthesis of Abemaciclib.* Organic Process Research & Development, 2017. **21**(9): 1447.
29. de Oliveira Silva, R.R., Cuesta Calvo, P.V., Fernandes da Silva, M., et al., *Flow Synthesis of a Thiazolidine Drug Intermediate in Capillary Microreactors.* Chemical Engineering & Technology, 2019. **42**(2): 465.
30. Pinheiro, D.d.S., Silva, R.R.d.O., Calvo, P.V.C., et al., *Microreactor Technology as a Tool for the Synthesis of a Glitazone Drug Intermediate.* Chemical Engineering & Technology, 2018. **41**(9): 1800.
31. Dubhashe, Y.R., Sawant, V.M., and Gaikar, V.G., *Process Intensification of Continuous Flow Synthesis of Tryptophol.* Industrial & Engineering Chemistry Research, 2018. **57**(8): 2787.
32. Armstrong, C.T., Pritchard, C.Q., Cook, D.W., et al., *Continuous flow synthesis of a pharmaceutical intermediate: a computational fluid dynamics approach.* Reaction Chemistry & Engineering, 2019. **4**(3): 634.
33. Singer, A.B., *Global Dynamic Optimization*. 2004, Massachusetts Institute of Technology.
34. Singer, A.B. and Barton, P.I., *Global solution of optimization problems with parameter-embedded linear dynamic systems.* Journal of Optimization Theory and Applications, 2004. **121**(3): 613.
35. Singer, A.B. and Barton, P.I., *Global Optimization with Nonlinear Ordinary Differential Equations.* Journal of Global Optimization, 2006. **34**(2): 159.
36. Singer, A.B., Taylor, J.W., Barton, P.I., and Green, W.H., *Global Dynamic Optimization for Parameter Estimation in Chemical Kinetics.* Journal of Physical Chemistry, 2006. **110**: 971.
37. Trampuž, M., Teslić, D., and Likozar, B., *Crystallization of fesoterodine fumarate active pharmaceutical ingredient: Modelling of thermodynamic equilibrium, nucleation, growth, agglomeration and dissolution kinetics and temperature cycling.* Chemical Engineering Science, 2019. **201**: 97.
38. Pohar, A. and Likozar, B., *Dissolution, Nucleation, Crystal Growth, Crystal Aggregation, and Particle Breakage of Amlodipine Salts: Modeling Crystallization Kinetics and Thermodynamic Equilibrium, Scale-up, and Optimization.* Industrial & Engineering Chemistry Research, 2014. **53**(26): 10762.
39. Schenk, C., Biegler, L.T., Han, L., and Mustakis, J., *Kinetic Parameter Estimation from Spectroscopic Data for a Multi-Stage Solid–Liquid Pharmaceutical Process.* Organic Process Research & Development, 2021. **25**(3): 373.
40. Su, Q., Nagy, Z.K., and Rielly, C.D., *Pharmaceutical crystallisation processes from batch to continuous operation using MSMPR stages: Modelling, design, and control.* Chemical Engineering and Processing: Process Intensification, 2015. **89**: 41.
41. Kraus, H.F., Acevedo, D., Wu, W., et al., *Kinetic modelling of an environmentally friendly carbamazepine synthesis via urea and iminostilbene in batch and continuous processes.* Reaction Chemistry & Engineering, 2023. **8**(2): 402.
42. Scale-up Systems Ltd., *Dynochem*. Scale-up Systems Ltd.
43. The MathWorks Inc., *MATLAB*. MathWorks.
44. Process Systems Enterprise, *gPROMS Process*. PSE.
45. Process Systems Enterprise, *gPROMS Formulated Products*. PSE.

View Article Online
DOI: 10.1039/D5RE00082C

46. Virtanen, P., Gommers, R., Oliphant, T.E., et al., *SciPy 1.0: fundamental algorithms for scientific computing in Python.* Nature Methods, 2020. **17**(3): 261.
47. Short, M., Biegler, L.T., García-Muñoz, S., and Chen, W., *Estimating variances and kinetic parameters from spectra across multiple datasets using KIPET.* Chemometrics and Intelligent Laboratory Systems, 2020. **203**: 104012.
48. Short, M., Schenk, C., Thierry, D., et al., *KIPET – An Open-Source Kinetic Parameter Estimation Toolkit.* Computer Aided Chemical Engineering, 2019. **47**: 299.
49. Beal, L.D.R., Hill, D., Martin, R.A., and Hedengren, J.D., *GEKKO Optimization Suite.* Processes, 2018. **6**(8).
50. Singer, A.B. and Barton, P.I., *Bounding the Solutions of Parameter Dependent Nonlinear Ordinary Differential Equations.* SIAM Journal on Scientific Computing, 2006. **27**(6): 2167.
51. COMSOL, *COMSOL Multiphysics*. COMSOL.
52. COMSOL, *Chemical Reaction Engineering Module*. COMSOL.
53. Burnham, S.C., Searson, D.P., Willis, M.J., and Wright, A.R., *Inference of chemical reaction networks.* Chemical Engineering Science, 2008. **63**(4): 862.
54. Tsu, J., Díaz, V.H.G., and Willis, M.J., *Computational approaches to kinetic model selection.* Computers & chemical engineering, 2019. **121**: 618.
55. August, E. and Papachristodoulou, A., *Efficient, sparse biological network determination.* BMC Systems Biology, 2009. **3**(25): 1752.
56. Taylor, C.J., Seki, H., Dannheim, F.M., et al., *An automated computational approach to kinetic model discrimination and parameter estimation.* React Chem Eng, 2021. **6**(8): 1404.
57. Willis, M.J. and Stosch, M.v., *Inference of chemical reaction networks using mixed integer linear programming.* Computers & Chemical Engineering, 2016. **90**: 31.
58. Akaike, H., *A new look at the statistical model identification.* IEEE Transactions on Automatic Control, 1974. **19**(6): 716.
59. Narisetty, N.N., *Chapter 4 - Bayesian model selection for high-dimensional data*, in *Handbook of Statistics*, A.S.R. Srinivasa Rao and C.R. Rao, Editors. 2020, Elsevier. p. 207.
60. Burnham, K.P., *Model selection and multimodel inference: a practical information-theoretic approach*. 2nd ed. ed, ed. D.R. Anderson and K.P. Burnham. 2002, New York: Springer.
61. Takebe, N., Naqash, A.R., O'Sullivan Coyne, G., et al., *Safety, Antitumor Activity, and Biomarker Analysis in a Phase I Trial of the Once-daily Wee1 Inhibitor Adavosertib (AZD1775) in Patients with Advanced Solid Tumors.* Clin Cancer Res, 2021. **27**(14): 3834.
62. Mortlock, A.A., Wilson, D.M., Kettle, J.G., et al., *5.02 - Selective Kinase Inhibitors in Cancer*, in *Comprehensive Medicinal Chemistry III*. 2017. p. 39.
63. Yamamoto, G., Tanaka, K., Kamata, R., et al., *WEE1 confers resistance to KRASG12C inhibitors in non-small cell lung cancer.* Cancer Letters, 2025. **611**: 217414.
64. Rodríguez-Vázquez, G.O., Diaz-Quiñones, A.O., Chorna, N., et al., *Synergistic interactions of cytarabine-adavosertib in leukemic cell lines proliferation and metabolomic endpoints.* Biomedicine & Pharmacotherapy, 2023. **166**: 115352.
65. Royal Society of Chemistry. *ChemSpider*. 2023 [cited 2023 10/03/2023]; Available from: http://www.chemspider.com/.
66. Kim, S., Chen, J., Cheng, T., et al., *PubChem 2023 update.* Nucleic Acids Research, 2023. **51**(D1): D1373.
67. Strieter, E.R., Bhayana, B., and Buchwald, S.L., *Mechanistic Studies on the Copper-Catalyzed N-Arylation of Amides.* Journal of the American Chemical Society, 2009. **131**(1): 78.
68. Ribas, X. and Güell, I., *Cu(I)/Cu(III) catalytic cycle involved in Ullmann-type cross-coupling reactions.* 2014. **86**(3): 345.

69. Sambiagio, C., Marsden, S.P., Blacker, A.J., and McGowan, P.C., *Copper catalysed Ullmann type chemistry: from mechanistic aspects to modern development.* Chemical Society Reviews, 2014. **43**(10): 3525.
70. Bunnett, J.F., *Mechanism and reactivity in aromatic nucleophilic substitution reactions.* Quarterly Reviews, Chemical Society, 1958. **12**(1): 1.
71. Kirby, A.J. and Varvoglis, A.G., *The reactivity of phosphate esters: reactions of monoesters with nucleophiles. Nucleophilicity independent of basicity in a bimolecular substitution reaction.* Journal of the Chemical Society B: Physical Organic, 1968: p. 135.
72. Cohen, T. and Cristea, I., *Kinetics and mechanism of the copper(I)-induced homogeneous Ullmann coupling of o-bromonitrobenzene.* Journal of the American Chemical Society, 1976. **98**(3): 748.
73. Oh, H.K., Ku, M.H., Lee, H.W., and Lee, I., *Nucleophilic Substitution Reactions of Aryl Dithioacetates with Pyridines in Acetonitrile.* The Journal of Organic Chemistry, 2002. **67**(11): 3874.
74. Kundu, A., Inoue, M., Nagae, H., et al., *Direct ortho-C–H Aminoalkylation of 2-Substituted Pyridine Derivatives Catalyzed by Yttrium Complexes with N,N'-Diarylethylenediamido Ligands.* Journal of the American Chemical Society, 2018. **140**(23): 7332.
75. Evano, G., Nitelet, A., Thilmany, P., and Dewez, D.F., *Metal-Mediated Halogen Exchange in Aryl and Vinyl Halides: A Review.* Frontiers in Chemistry, 2018. **6**: 114.
76. Jin, X. and Davies, R.P., *Copper-catalysed aromatic-Finkelstein reactions with amine-based ligand systems.* Catalysis Science & Technology, 2017. **7**(10): 2110.
77. Klapars, A. and Buchwald, S.L., *Copper-Catalyzed Halogen Exchange in Aryl Halides: An Aromatic Finkelstein Reaction.* Journal of the American Chemical Society, 2002. **124**(50): 14844.
78. Pace, R.D. and Regmi, Y., *The Finkelstein Reaction: Quantitative Reaction Kinetics of an SN2 Reaction Using Nonaqueous Conductivity.* Journal of Chemical Education, 2006. **83**(9): 1344.
79. Surry, D.S. and Buchwald, S.L., *Diamine ligands in copper-catalyzed reactions.* Chemical Science, 2010. **1**(1): 13.
80. DECHEMA. *DETHERM*. [accessed 05/10/2022]; Available from: https://detherm.cds.dechema.de/.
81. Tao, M., Wang, Z., Gong, J., et al., *Determination of the Solubility, Dissolution Enthalpy, and Entropy of Pioglitazone Hydrochloride (Form II) in Different Pure Solvents.* Industrial & Engineering Chemistry Research, 2013. **52**(8): 3036.
82. Keizer, J., *Diffusion effects on rapid bimolecular chemical reactions.* Chemical Reviews, 1987. **87**(1): 167.
83. Awaji, A.I., Köksoy, B., Durmuş, M., et al., *Novel Hexadeca-Substituted Metal Free and Zinc(II) Phthalocyanines; Design, Synthesis and Photophysicochemical Properties.* Molecules, 2019. **24**(1).
84. Dutt, G.B. and Periasamy, N., *Electron-transfer distance in intermolecular diffusion-limited reactions.* Journal of the Chemical Society, Faraday Transactions, 1991. **87**(24): 3815.
85. Waite, T.R., *General Theory of Bimolecular Reaction Rates in Solids and Liquids.* The Journal of Chemical Physics, 1958. **28**(1): 103.
86. Collins, F.C. and Kimball, G.E., *Diffusion-controlled reaction rates.* Journal of Colloid Science, 1949. **4**(4): 425.
87. Shaydullin, R.R., Galushko, A.S., Ilyushenkova, V.V., et al., *Are activation barriers of 50–70 kcal mol−1 accessible for transformations in organic synthesis in solution?* Chemical Science, 2025. **16**(12): 5289.
88. Ouellette, R.J. and Rawn, J.D., *3 - Introduction to Organic Reaction Mechanisms*, in *Organic Chemistry (Second Edition)*, R.J. Ouellette and J.D. Rawn, Editors. 2018, Academic Press. p. 51.

89. Espie, D.M., *The use of nonlinear parameter estimation for dynamic chemical reactor modelling*. 1987, University of London.
90. Pritchard, D.J. and Bacon, D.W., *Statistical assessment of chemical kinetic models.* Chemical engineering science, 1975. **30**(5): 567.
91. McLean, K.A.P. and McAuley, K.B., *Mathematical modelling of chemical processes—obtaining the best model predictions and parameter estimates using identifiability and estimability procedures.* The Canadian Journal of Chemical Engineering, 2012. **90**(2): 351.
92. Banks, H.T. and Joyner, M.L., *AIC under the framework of least squares estimation.* Applied Mathematics Letters, 2017. **74**: 33.
93. Kletting, P. and Glatting, G., *Model selection for time-activity curves: The corrected Akaike information criterion and the F-test.* Zeitschrift für Medizinische Physik, 2009. **19**(3): 200.
94. Rodman, A.D. and Gerogiorgis, D.I., Parameter estimation and sensitivity analysis for dynamic modelling and simulation of beer fermentation. Computers & Chemical Engineering, 2020. **136**: 106665.
95. Pilarski, D.W. and Gerogiorgis, D.I., *Systematic Parameter Estimation And Dynamic Simulation of Cold Contact Fermentation for Alcohol-Free Beer Production*, Processes, 2022. **10**(11), 2400.

Reaction Kinetics for the Synthesis of an Anti-cancer Drug (Adavosertib) Precursor

View Article Online
DOI: 10.1039/D5RE00082C

Matthew Blair[a], Mazaher M. Chalchooghi[b], Robert J. Cox[b], Dimitrios I. Gerogiorgis[a,*]

[a]Institute for Materials and Processes (IMP), School of Engineering, University of Edinburgh, The King's Buildings, Edinburgh, EH9 3FB, United Kingdom

[b]Chemical Development, Pharmaceutical Technology and Development, Operations, AstraZeneca, Macclesfield, SK10 2NA, United Kingdom

DATA AVAILABILITY STATEMENT

A legal confidentiality agreement (2020) is in effect and has been signed between the University of Edinburgh and AstraZeneca plc, governing the publication of results (under the auspices of the Engineering & Phys. Sciences Research Council, EPSRC). Tabulated, literature reference and digitised reaction (concentration) data are all provided and suffice for the reproduction of all Figs./results presented in the article. Specific requests for original (raw) experimental data and/or the software (MATLAB®) code by Mr M. Blair can be considered in writing, to ensure the above is not violated.